International Conference on Space Optics—ICSO 2010

Rhodes Island, Greece

4–8 October 2010

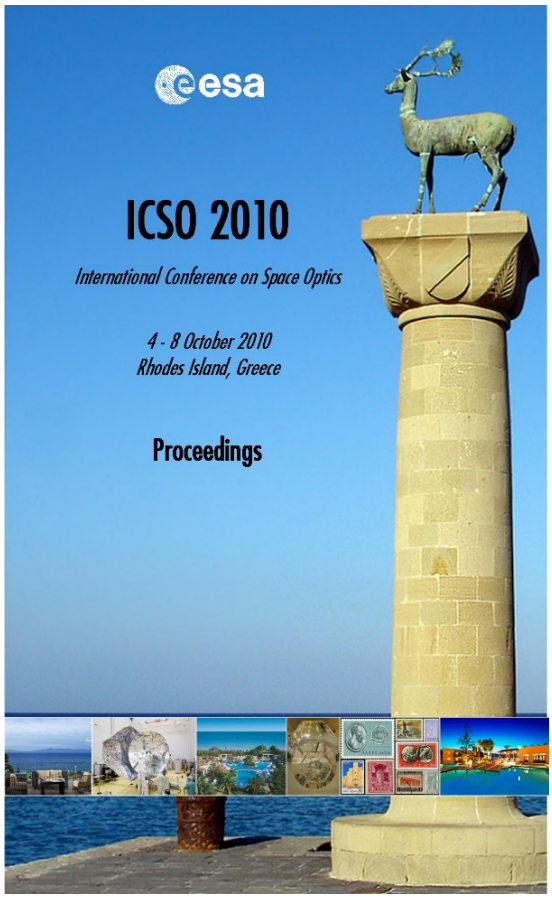

Edited by Errico Armandillo, Bruno Cugny, and Nikos Karafolas

The solar-orbiter EUI instrument optical developments

J.-P. Halain, Y. Houbrechts, F. Auchère, P. Rochus, et al.

International Conference on Space Optics — ICSO 2010, edited by Errico Armandillo, Bruno Cugny, Nikos Karafolas, Proc. of SPIE Vol. 10565, 1056561 · © 2010 ESA and CNES
CCC code: 0277-786X/17/$18 · doi: 10.1117/12.2552542

THE SOLAR-ORBITER EUI INSTRUMENT OPTICAL DEVELOPMENTS,

J.-P. Halain[1], Y. Houbrechts[1], F. Auchère[2], P. Rochus[1], T. Appourchaux[2], D. Berghmans[3], U. Schühle[4], L. Harra[5], E. Renotte[1], A. Zukhov[3]

[1]Centre Spatial de Liège, Liege Science Park, 4013 Angleur, Belgium.[2]Institut d'Astrophysique Spatiale, Orsay, France. [3]Royal Observatory of Belgium, Avenue Circulaire, Uccle, Belgium. [4]Max-Planck-Institut für Sonnensystemforschung, Lindau, Germany. [5]Mullard Space Science Laboratory, Surrey RH5 6NT, UK

I. THE EUI INSTRUMENT:

The Solar Orbiter mission [1],[2],[3], part of the Cosmic Vision Science Program of European Space Agency (ESA), to be launched in 2017, is devoted to the Sun observation. From its unique vantage point in an elliptical orbit around the Sun, and approaching as close as 60 solar radii, Solar Orbiter will provide unprecedented close-up and high-latitude observations of the Sun. The Extreme Ultraviolet Imager (EUI) instrument [4],[5],[6],[7],[8],[9] was selected as one of the 10 scientific payload instruments of the Solar Orbiter mission.

The EUI instrument is composed of two high-resolution imagers (HRI), one observing the hydrogen Lyman-α line (1216 Å) and one the extreme ultra-violet (EUV) band 174 Å, and one dual band full-sun imager (FSI) working alternatively at the two 174 Å and 304 Å passbands. The HRI channels use a two-mirror Ritchey–Chrétien off-axis optical system, and the FSI uses a single mirror off-axis Herschelian system. The normal-incidence telescopes are in co-alignment and operate independently. Their mirrors have optimized coatings for FUV or EUV reflectivity in each passband. The spectral selection is complemented with filters and filter wheel rejecting the visible and infrared radiation.

Fig.1 shows the functional diagram of the HRI and FSI telescopes, including the front filter and its protection mechanism (door) and entrance baffle, the EUV filter wheel mechanisms and telescope (i.e. mirrors), the detector and proximity electronic acquisition chain, and the common electronic box. The EUI channels are mounted on a common optical bench structure (Figure2) supported by a set of dedicated mounts.

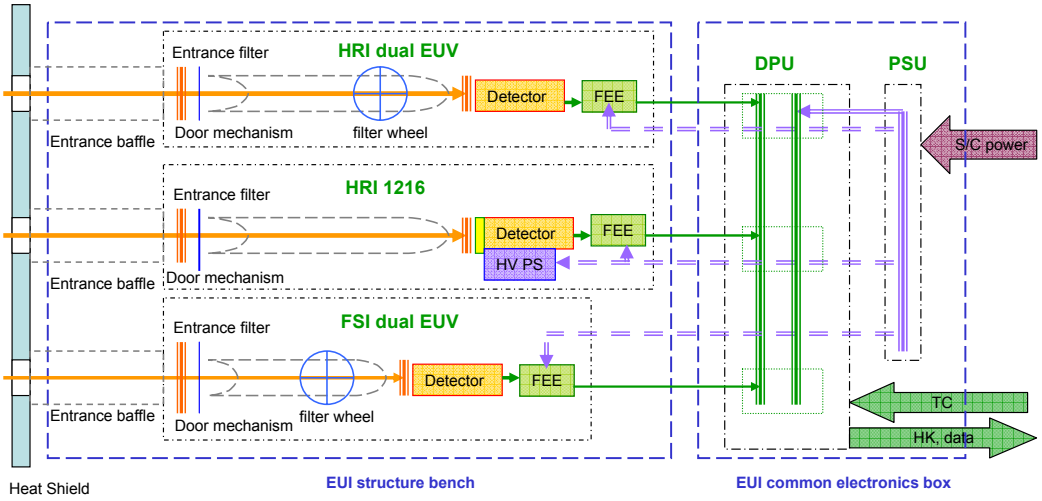

Fig.1. EUI functional diagram

Table 1 lists the intended temporal and spatial resolutions, field-of-view (FOV) as well as passbands of the EUI instrument.

Table 1. EUI main parameters

Parameter			Values
EUI	FSI_{dual}	Passband centre	174 Å and 304 Å alternatively
		Field of View	5.2 arcdeg × 5.2 arcdeg
		Angular resolution (2 px)	9 arcsec
	HRI_{EUV}	Passband centre	174 Å
		Field of View	1000 arc sec square
		Angular resolution (1 px)	0.5 arcsec
	$HRI_{Ly-\alpha}$	Passband centre	1216 Å
		Field of View	1000 arcsec square
		Angular resolution (2 px)	1 arcsec

The EUI channels are mounted on a common optical bench structure (Fig. 2) supported by a set of dedicated mounts. The optical bench structure is made out of a CFRP sandwich panel with an aluminum honeycomb core for stiffness and thermal stability; and the optical channels are covered by CFRP facesheet panels. The common electronics box (CEB) is a separate unit (Fig. 3) providing control of the mechanisms (filter wheels and doors);, containing the processing unit, and ensuring the electrical interface with the spacecraft. The mechanical configuration has been improved to fit the spacecraft volume constraints. The mounts will minimize thermal and mechanical couplings between EUI and platform, and provide sufficient stiffness to guarantee a sufficiently high first eigenfrequency.

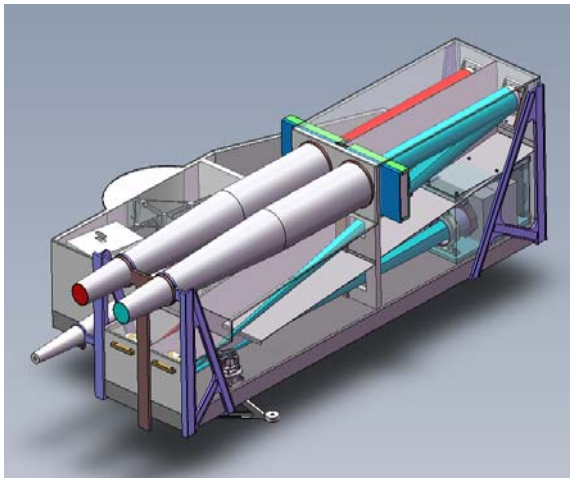

Fig.2. EUI optical bench configuration

Fig.3. EUI common electronic box

II. OPTICAL DESIGN:

A. HRI channels

The two HRI channels share a quasi-identical optical design based on an off-axis Gregory telescope optimized in length and width (Fig.4), with an entrance pupil located at the front section of an entrance baffle. The HRI entrance baffle is designed to provide a reduction of the heat input reaching the entrance foil filter and a first level of protection against straylight from the overall solar disk. An entrance filter is inserted between the entrance pupil and the primary mirror to provide protection against excessive heat input and an efficient visible light rejection. The reflective coatings of the mirrors are optimized for the selected spectral passbands. The HRI channel uses a 2k x 2k APS detector.

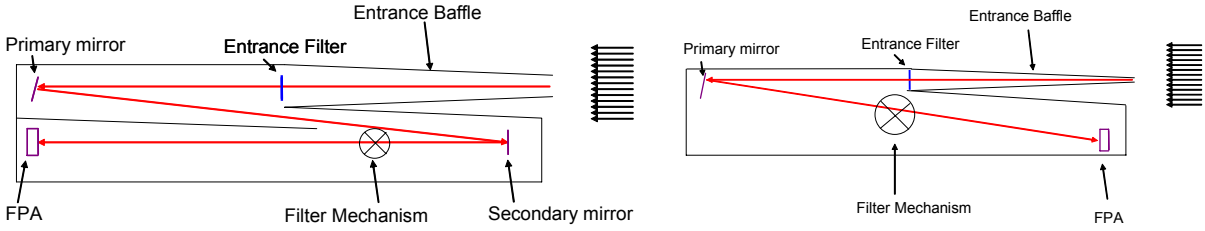

Fig.4. HRI and FSI optical design

B. FSI channel

The FSI channel [4] is based upon a single off-axis mirror, Herschelian telescope (Fig.4), making an image of a 3.6 deg x 3.6 deg FOV through a 5-mm entrance pupil located at 700 mm from the mirror with an equivalent focal length of 450mm. An entrance filter is positioned 310 mm behind the entrance pupil to reject visible and IR light. The wavebands are selected using bandpass filters mounted on a filter wheel and reflective coatings on the mirror. The FSI channel uses a 3k x 3k APS detector.

III. DEVELOPMENTS:

A. Entrance baffles

The heat protection of the HRI channels is based on optical reflective baffles to limit the heat load entering the instrument. The HRI entrance baffle is designed to reject a maximum of the incoming sunlight, i.e. more than 65% even for large offset angles of the spacecraft pointing. The FSI entrance baffle is black inside, and simply

absorbs the low power incoming through its small entrance pupil. The EUI baffles are completed by a thermal diaphragm and a front mirror, located between the spacecraft heat shield and the baffles, to reduce the heat load on the area surrounding the entrance pupils.

The design of the HRI entrance baffle is based on a spherical heat rejection mirror (HRM), located at 500 mm of the entrance pupil, and on the specular entrance filter. A specific reflective tube has been added to reject the heat load out of the baffle through the entrance pupil. Ray tracing analyses (Fig.5) show that the incoming solar rays are reflected outside the baffle with at most three reflections, for an off-pointing angle up to 1.25 arcdeg. A rejection rate of 77% is computed for a zero off-pointing (-and 78.2% for an off-pointing of 1.25 arcdeg, assuming 90% reflection on the HRM and 80% on the baffle tube. The rejection rate highly depends on the filter absorption assumed in the model, and baffle internal reflectivity.

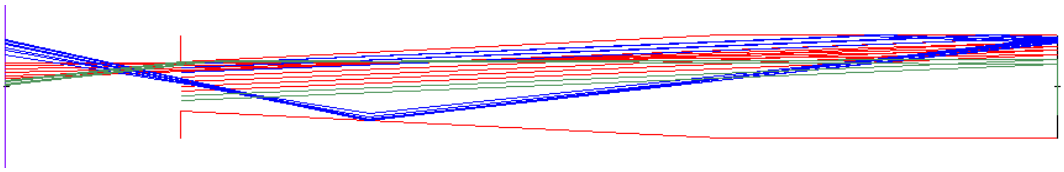

Fig.5. HRI entrance baffle ray-tracing simulation

In order to validate the thermo-optical model of the HRI entrance baffle, a prototype has been tested to correlate the model using measured diffuse and specular reflectivities of the HRM/dummy filter and the tube/cylinder. A second prototype will be made to validate the manufacturing challenge of a CFRP tube with Aluminum internal coating.

B. Transmission filters

In each EUI channel, the light enters the instrument through an entrance filter. The HRI_{EUV} and FSI channels are using aluminum filters that suppress most of the UV, visible and IR counterparts of the solar radiation, which is of primary importance to avoid over-heating the primary mirror. The $HRI_{Ly\alpha}$ entrance filter is a broad-band interference filter which rejects visible and infrared light as well as EUV and X-rays.

A second bandpass selection filter is used in the HRI_{EUV} to ensure spectral purity, and is mounted on a filter wheel allowing redundancy. Band selection filters is also used in the FSI channel to select one or the other of the two bands reflected by the mirrors. These EUV filters are very thin and mounted on filter wheels. A narrow-band filter is used in the $HRI_{Ly\alpha}$ to isolate the Lyman-α line in the solar spectrum with 95% spectral purity.

Baseline materials identified for the EUV filters are Aluminum for the entrance filters and Al/Zr for (short wavelengths) and Al/Mg/Al (longer wavelengths) for the band selection filters. Such filters are available commercially with long flight heritage. Specially designed entrance filters are however required to sustain the high thermal load they will have to endure. A custom mesh and grid support is therefore considered. The supporting structure (mesh and grid) will be made, in-house, with an electrolytic process. A growth initiating layer (copper) is deposited on the multilayers filter membrane with a manufacturing guide that can have any shape (hexagonal for example). The grid material (Nickel) is then grown within the guide that is removed at the end of the process. Such filter prototypes are under development (Fig. 6)

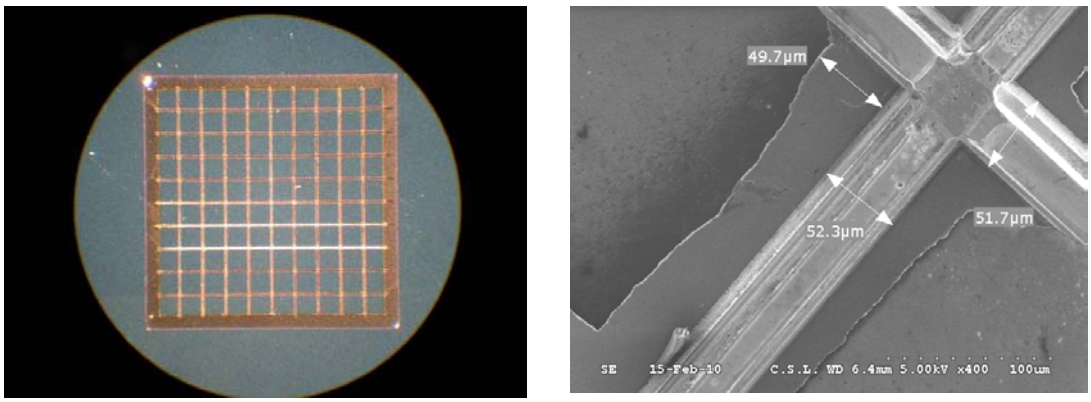

Fig.6. Filter grid prototype

C. Mirror coatings

The Classical approach to have multiple wavelengths channel is to apply several coatings on the mirrors and select the wavelength with rotating mask (as in EVE/SDO and EUVI/STEREO). For the FSI channel, we

propose a new approach (Fig.7) of a multiple-band coating on the mirror and filter wheel for wavelength selection, allowing a smaller aperture (reduced heat input and mass).

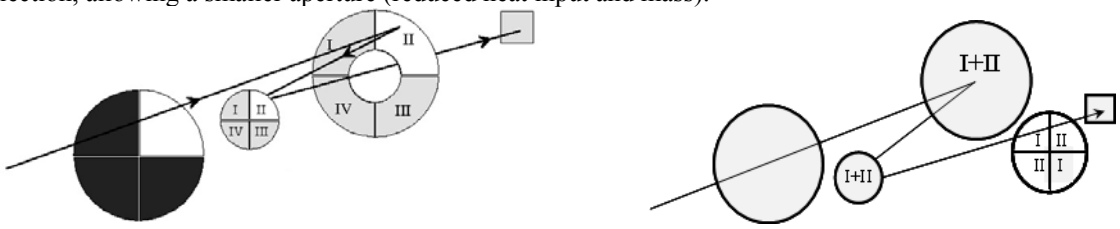

Fig.7. Classical and new approach of multiple band channel

The HRI_{EUV} and FSI channels are based on innovative multilayer coatings (Fig.8). For HRI, the coating will allow the transmission of 2 bands centered on 174 Å (Fe X) and 335 Å (Fe XVI); for FSI, it will allow the transmission of 2 bands centered on 174 Å (Fe X) and 304 Å (He II); with the rejection of several bright unwanted spectral lines (e.g. Fe XII 195 Å and Fe XVI 335 Å). These multilayers are undergoing an extensive ageing study to be qualified for the Solar Orbiter mission. The coatings make use of barrier layers to stabilize the multilayer structure. Thermal cycling between -50°C and + 70°C and exposition to warm water vapor have demonstrated that these new multilayers are very stable and should not degrade during the mission. For example, no variation in reflectivity was found after testing on the 304 Å B4C/Mo/Si coating produced for the Herschel NASA sounding rocket [10].

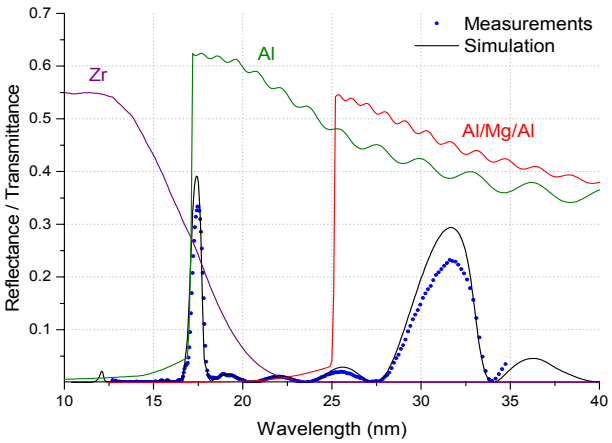

Fig.8. Transmittances of the front and focal plane filters and reflectance of dual passband 174/304 Å multilayer coating. Black curves: theoretical reflectances, blue dots: measurements. Green, purple and red curves: entrance Al filter, focal plane Zr and Al/Mg/Al filters

The Lyman-α channel mirrors use proven technology for the coatings of the primary and secondary mirrors. The Al/MgF2 (aluminum/magnesium fluoride) coating provides reflectivity at 1216 Å over 75%. This optical design provides a high throughput by using a narrow-band and a broadband interference filter on MgF2 substrate to isolate the spectral line at 1216 Å (that is moreover the brightest UV line of the solar emission spectrum).

D. Detectors

The baseline detectors for the three EUI channels are back-thinned CMOS Active Pixel Sensors with 2k x 2k format for HRI channels and 3k x 3k format for the FSI, providing a pixel resolution of 0.5 arcsec and 4.5 arcsec respectively. The APS solution provides rolling or global electronic shutter operation capability, and avoids the need for a mechanical shutter, and by design is a radiation hard detector with limited cooling (-40°C).

A dedicated detector development has been started in 2009, with low noise and high EUV QE requirement, and will result in a 256x256 sensor containing 16 test pixel variants organized in blocks of 64x64 pixels, and a 1024x1024 sensor containing the best guess pixel variant. These detector prototypes will be tested in EUV and under radiation by the end of 2010. The objective is to demonstrate the suitability of the back-illuminated thinned CMOS-APS technology as very low noise EUV detector and to confirm radiation tolerance of APS. These prototypes will then serve to select the best pixel design to be used for the flight devices. The required low noise and high dynamic range are obtained by combining multiple readouts on low and high gain output channels. The EUV sensitivity is obtained by back-thinning a processed Silicon On Insulator (SOI) wafer, with epitaxial layer thickness of 3µm, on which the CMOS circuits are deposited (0.18 CIS process).

The Lyman-α detector will use the same sensor and readout electronic circuits. However, for better sensitivity at the Lyman-α wavelength, and for better suppression of solar continuum outside the filter pass band, the sensor will be mated with an image intensifier. The Lyman-α channel has indeed no metal filters like the EUV channels providing sufficient blocking of visible Sun light, but interference filters which need additional visible light blocking. This is accomplished by a blocking filter inside the MCP-intensifier, making it a solar-blind detector. The intensifier will use multichannel plates with a photocathode coating and the anode will be coupled

to the sensor with a fiber optic taper, to reduce the image size to the sensor size. A breadboard model of such detector has been built and another prototype is under development for mechanical design space qualification.

V. CONCLUSIONS AND ACKNOWLEDGEMENTS:

The Solar Orbiter ambitious characteristics draw severe constraints on the EUI instrument design. The EUI optical design thus relies on developments of dedicated transmission filters, multilayers coating and specific detectors.

The EUI instrument is developed in a collaboration which includes the Centre Spatial de Liège and Royal Observatory of Belgium (Belgium), the Institut d'Astrophysique and Institut d'Optique (France), the UCL Mullard Space Science Laboratory (UK), and Max Planck Institute for Solar System Research (Germany). The Belgian institutions are funded by Belgian Federal Science Policy Office; the French institutions by Centre National d'Etudes Spatiales (CNES), the UK institution by the UK Space Agency (UKSA); and the German institution by Deutsche Zentrum für Luft- und Raumfahrt e.V. (DLR).

REFERENCES:

[1] Fleck B., Harrison R. A., Marsden R. G., Wimmer-Schweingruber R., "Summary of the Solar Orbiter payload working group activities, Telescopes and Instrumentation for Solar Astrophysics", Proc. SPIE 5171, 123-130 (2004).

[2] Marsden R.G., Marsch E. and the Solar Orbiter Science Definition Team, "Solar Orbiter Science Requirements Document", SCI-SH/2005/100/RGM Issue 1 Revision 2 (2005).

[3] Mc Coy D., and the Solar Orbiter assessment team, "Solar Orbiter Payload Definition Document", SCI-A/2004/175/AO Issue 5 Revision 0 (2006).

[4] Auchere F., Song X., Rouesnel F., Appourchaux T., Fourmon J.-J., Le Clec'h J.-C., Berthe M., Defise J.-M., Mazy, E., Rochus P., Mercier R., Ravet M.-F., "Innovative designs for the imaging suite on Solar Orbiter, Solar Physics and Space Weather Instrumentation", Proc. SPIE 5901, 298-304 (2005).

[5] Vial J.-C., "Solar Orbiter: A unique opportunity for investigating small-scale physical processes at work in the magnetic solar atmosphere, Advances in Space Research", Advances in Space Research, 36, 1375-1386 (2005).

[6] Young P. R., and the EUS Science Working Group, "Science With The Extreme Ultraviolet Spectrometer For Solar Orbiter", Proc. of The Second Solar Orbiter Workshop 641 (2006).

[7] Rochus P., Halain J.P., Renotte E., Berghmans D., Zhukov A., Hochedez J.F., Appourchaux T., Auchère F., Harra L.K, Schühle U., Mercier R.., "The Extreme Ultraviolet Imager (EUI) on-board the Solar orbiter Mission", 60th International Astronautical Congress (2009).

[8] Hochedez J.-F., Schühle U., Pau J. L., Alvarez J., Hainaut O., Appourchaux T., Auret F., Belsky A., Bergonzo P., Castex M. C., Deneuville A., Dhez P., Fleck B., Haenen K., Idir M., Kleider J.-P., Lefeuvre E., Lemaire P., Monroy E., Muret P., Munoz E., Nesladek M., Omnes F., Pace E., Peacock A. J., Van Hoof C. A., "New UV detectors for solar observations", Innovative Telescopes and Instrumentation for Solar Astrophysics. Edited by Stephen L. Keil, Sergey V. Avakyan . Proc SPIE 4853, 419-426 (2003).

[9] Hochedez J.-F., Appourchaux T., Defise J.-M., Harra L. K., Schuehle U., Auchère F., Curdt W., Hancock B., Kretzschmar M., Lawrence G., Marsch E., Parenti S., Podladchikova E., Rochus P., Rodriguez L., Rouesnel F., Solanki S., Teriaca L., Van Driel L., Vial J.-C., Winter B., Zhukov A., "EUI, The Ultraviolet Imaging Telescopes of Solar Orbiter", The Second Solar Orbiter Workshop (2006).

[9] Auchère F., Ravet-Krill M.-F., Moses J.D., Rouesnel F., Moalic J.-P., Barbet D., Hecquet C., Jérome A., Mercier R.; Leclec'h J.-C., Delmotte F., Newmark J.S., "HECOR, a HElium CORonagraph aboard the Herschel sounding rocket", Proc. SPIE, 6689, 66890A-66890A-11 (2007).